Kinematic and Dynamic Analyses of Planar 3 Degree of Freedom Hopping Robot

February 26, 2018

Contents

1 Introduction **1**
- 1.1 Motivation . . . 1
- 1.2 Proof: mobility . . . 2

2 Forward kinematics **2**
- 2.1 Open sub-chain forward kinematics . . . 2
- 2.2 Numerical forward kinematics for a closed-chain robot . . . 3
  - 2.2.1 Newton-Raphson root-finding method . . . 3
  - 2.2.2 Loop-closure equations . . . 3
  - 2.2.3 Constraint Jacobian . . . 4
  - 2.2.4 Numerical forward kinematics algorithm . . . 4
- 2.3 Actuation requirements . . . 4
  - 2.3.1 Actuator Jacobians . . . 4
  - 2.3.2 Motor sizing . . . 6

3 Inverse Kinematics **6**
- 3.1 θ-chain inverse kinematics . . . 7
- 3.2 ψ-chain inverse kinematics . . . 8
- 3.3 ϕ-chain inverse kinematics . . . 9

1 Introduction

1.1 Motivation

We want to design a closed-chain robot to study legged locomotion. A closed-chain legged robot has more mass concentrated at its top, compared to an open-chain robot. This is advantageous for legged locomotion for two reasons:

- Less mass near the foot increases agility and reduces actuation requirements at the hip.
- The robot behaves like an inverted pendulum during stance, so concentrating the mass at the top of the pendulum increases stability.

The remainder of this paper derives a mathematical model of a particular planar 3-degree-of-freedom (DOF) closed-chain robot. Having 3 DOF is desirable because a planar legged robot with 3 DOF can fully control its position and orientation during stance and flight. [1]

These analyses closely follow [1], especially Chapters 6 ("Inverse Kinematics") and 7 ("Kinematics of Closed Chains").

[1] The interface between the foot and ground can be viewed as an unactuated joint, inviting questions about underactuation and controllability for this particular robot.

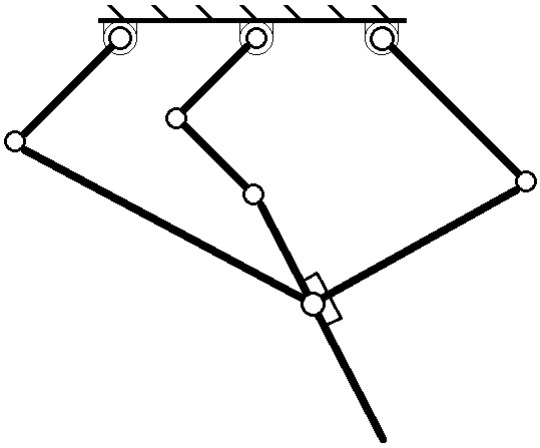

Figure 1: Schematic diagram of the planar robot.

1.2 Proof: mobility

This proof is simply a verification that the robot shown in Figure 1 has 3 degrees of freedom, using Grübler's formula:

$$\text{DOF} = m(N - 1 - J) + \sum_{i=1}^{J} f_i, \tag{1}$$

where $m = 3$ for planar mechanisms, N is the number of links (including the base), J is the number of joints, and f_i is the number of freedoms at the i^{th} joint. From Figure 1, $N = 8$, $J = 9$, and $f_i = 1$ for all i. Note that the lowest joint in the figure is really two joints; one joint connects the left coupler to the middle link, and the other connects the right coupler to the middle link. Thus, according to Grübler's formula, the robot has 3 degrees of freedom.

2 Forward kinematics

Closed-chain linkages can be decomposed into groups of open-chain linkages (hereafter referred to as "open sub-chains") whose motions are constrained by loop-closure equations. Our robot comprises three open sub-chains, shown in Figure 2: the θ-chain is on the left, the ϕ-chain is in the middle, and the ψ-chain is on the right. We will first examine the forward kinematics for each open sub-chain and then develop loop-closure equations.

2.1 Open sub-chain forward kinematics

The forward kinematics of each open sub-chain relate the foot frame $\{f\}$ to the base frame $\{b\}$. The forward kinematics of the θ-chain are

$$\begin{bmatrix} x_f \\ y_f \\ \measuredangle_f \end{bmatrix} = \begin{bmatrix} -b_1 + l_1 \cos\theta_1 + l_2 \cos(\theta_1 + \theta_2) + l_8 \cos(\theta_1 + \theta_2 + \theta_3) \\ l_1 \sin\theta_1 + l_2 \sin(\theta_1 + \theta_2) + l_8 \sin(\theta_1 + \theta_2 + \theta_3) \\ \theta_1 + \theta_2 + \theta_3 \end{bmatrix}. \tag{2}$$

The forward kinematics of the ϕ-chain are

$$\begin{bmatrix} x_f \\ y_f \\ \measuredangle_f \end{bmatrix} = \begin{bmatrix} l_3 \cos\phi_1 + l_4 \cos(\phi_1 + \phi_2) + (l_7 + l_8) \cos(\phi_1 + \phi_2 + \phi_3) \\ l_3 \sin\phi_1 + l_4 \sin(\phi_1 + \phi_2) + (l_7 + l_8) \sin(\phi_1 + \phi_2 + \phi_3) \\ \phi_1 + \phi_2 + \phi_3 \end{bmatrix}. \tag{3}$$

Lastly, the forward kinematics of the ψ-chain are

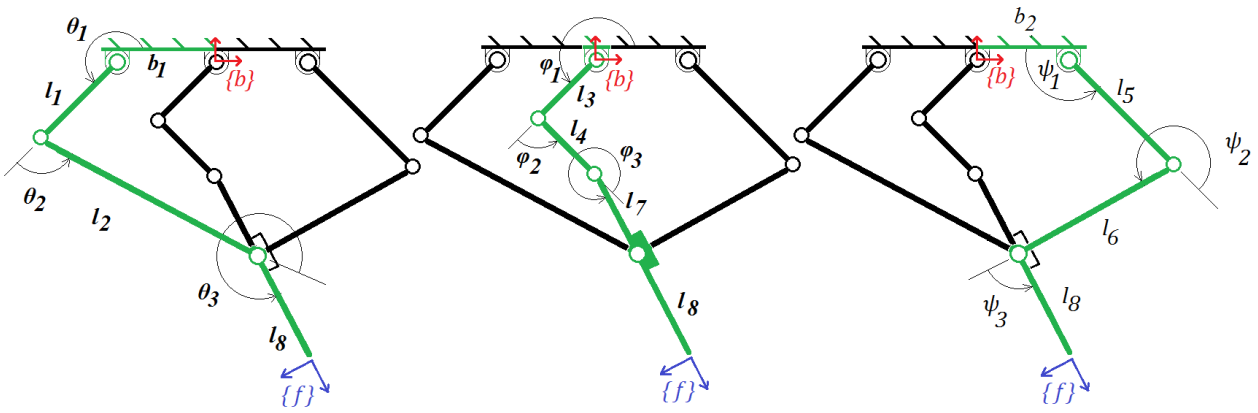

Figure 2: The planar robot comprises three open sub-chains, referred to as the θ-, ϕ-, and ψ-chains, from left to right.

$$\begin{bmatrix} x_f \\ y_f \\ \measuredangle_f \end{bmatrix} = \begin{bmatrix} b_2 + l_5 \cos\psi_1 + l_6 \cos(\psi_1 + \psi_2) + l_8 \cos(\psi_1 + \psi_2 + \psi_3) \\ l_5 \sin\psi_1 + l_6 \sin(\psi_1 + \psi_2) + l_8 \sin(\psi_1 + \psi_2 + \psi_3) \\ \psi_1 + \psi_2 + \psi_3 \end{bmatrix}. \tag{4}$$

Thus, if we know the joint positions of any of the three open sub-chains, we can calculate the end-effector pose. Although this formulation is straightforward, it is not particularly useful on its own, because both the actuated and unactuated joint positions in that chain must be known in order to calculate the end-effector pose. It would be more useful to have a mapping from the positions of only the actuated joints to the end-effector pose.

One way to develop such a mapping is to first solve for the unactuated joint positions as functions of the actuated joint positions, using loop closure equations. Then, once all the joint positions are known, we can choose any of the three open sub-chains and use the corresponding forward kinematics equations to calculate the end-effector pose.

2.2 Numerical forward kinematics for a closed-chain robot

The forward kinematics method described above requires solving a system of nonlinear equations (with potentially many solutions), so a numerical root-finding algorithm may be more appropriate than seeking an analytical solution. One such algorithm is the Newton-Raphson method.

2.2.1 Newton-Raphson root-finding method

Consider a nonlinear equation $g(q) = \ldots$, for which we seek the roots, i.e., we wish to solve $g(q) = 0$. Linearize the equation by writing a Taylor series expansion of $g(q)$ about the point q_0:

$$g(q) = g(q_0) + \left.\frac{\partial g}{\partial q}\right|_{q_0} (q - q_0) + \text{h.o.t.} \tag{5}$$

Discarding the higher-order terms, the roots are approximately

$$q = q_0 - \left(\left.\frac{\partial g}{\partial q}\right|_{q_0} \right)^{-1} g(q_0) \quad . \tag{6}$$

Taking the new q as q_0, this method can be iterated until some convergence threshold criterion is satisfied.

2.2.2 Loop-closure equations

Refer to Figures 1 and 2 and observe that the open sub-chains intersect at a common joint, measured by θ_3 and ψ_3. Consequently, there are three loops: the θ-ϕ loop, the ϕ-ψ loop, and the ψ-θ loop. We can describe these three loops with two sets of equations:

$$g(\theta, \phi, \psi) := \begin{bmatrix} T_{bf}(\theta) - T_{bf}(\phi) \\ -T_{bf}(\phi) + T_{bf}(\psi) \end{bmatrix} = \begin{bmatrix} 0 \\ 0 \end{bmatrix} \tag{7}$$

where $T_{bf}(\cdot)$ represents the twist from the base frame $\{b\}$ to the end-effector frame $\{f\}$ along the corresponding open sub-chain; this is just a compact representation of the earlier open sub-chain forward kinematic equations, so the left and right sides of the equation are 6×1 column vectors.

For a given set of actuated joint angles $q_a = [\theta_1, \phi_1, \psi_1]^{\mathrm{T}}$, we seek unactuated joint angles ($q_u = [\theta_2, \theta_3, \phi_2, \phi_3, \psi_2, \psi_3]^{\mathrm{T}}$), i.e., the roots of the loop-closure equations, so the iterative Newton-Raphson root-finding equation is

$$\left[\theta_2^{k+1}, \theta_3^{k+1}, \phi_2^{k+1}, \phi_3^{k+1}, \psi_2^{k+1}, \psi_3^{k+1}\right]^{\mathrm{T}} = q_u^{k+1} = q_u^k - J_c^{-1} g\left(q_a, q_u\right) \ , \tag{8}$$

where J_c, the *constraint Jacobian*, is the matrix of partial derivatives of the loop-closure expression with respect to the elements of q_u. Since the loop-closure equation was expressed as a 6×1 column vector, the constraint Jacobian is a square 6×6 matrix.

2.2.3 Constraint Jacobian

As mentioned earlier, the constraint Jacobian J_c is the matrix of partial derivatives of the loop-closure expression with respect to the unactuated joint positions q_u. Differentiating the loop-closure equation above, we get the following 6×6 matrix:

$$J_c = \begin{bmatrix} \frac{\partial T_{bf}(\theta)}{\partial \theta_2} & \frac{\partial T_{bf}(\theta)}{\partial \theta_3} & -\frac{\partial T_{bf}(\phi)}{\partial \phi_2} & -\frac{\partial T_{bf}(\phi)}{\partial \phi_3} & 0 & 0 \\ 0 & 0 & -\frac{\partial T_{bf}(\phi)}{\partial \phi_2} & -\frac{\partial T_{bf}(\phi)}{\partial \phi_3} & \frac{\partial T_{bf}(\psi)}{\partial \psi_2} & \frac{\partial T_{bf}(\psi)}{\partial \psi_3} \end{bmatrix} . \tag{9}$$

2.2.4 Numerical forward kinematics algorithm

Now that we have the constraint Jacobian, we can develop an iterative numerical forward kinematics algorithm.

Algorithm 1 Newton-Raphson algorithm for closed-chain forward kinematics

function NRFK(q_a, q_u^0, ε) ▷ compute end-effector pose T_{bf} from actuated joint positions
  Initialize $r > \varepsilon$ ▷ measure of convergence
  while $r > \varepsilon$ **do** ▷ convergence threshold
    $q_u^{new} = q_u^0 - J_c^{-1} g\left(q_a, q_u^0\right)$
    $r = \frac{\left|g(q_a, q_u^0) - g(q_a, q_u^{new})\right|}{|g(q_a, q_u^0)|}$ ▷ update measure of convergence
    $q_u^0 = q_u^{new}$
  end while ▷ we now have approximate values for q_u
  $\theta = \begin{bmatrix} q_a(1) & q_u^{new}(1) & q_u^{new}(2) \end{bmatrix}^{\mathrm{T}}$
  return $\begin{bmatrix} x_f & y_f & \measuredangle_f \end{bmatrix}^{\mathrm{T}} = T_{bf}(\theta)$ ▷ $T_{bf}(\theta)$ is the end-effector pose computed using the θ-chain
end function

In summary, this algorithm finds approximate unactuated joint positions from the actuated joint positions and uses the positions along one open sub-chain to compute the end-effector pose. Note that this algorithm uses the θ-chain to compute the end-effector pose, but the other open sub-chains are equally viable.

2.3 Actuation requirements

We would now like to solve the inverse dynamics problem: what motor speeds/torques are required to generate a desired end-effector speed/force? This problem can be solved using the *actuator Jacobian*.

2.3.1 Actuator Jacobians

The actuator Jacobian maps generalized actuator velocities and forces to end-effector velocities and forces. Returning to the loop-closure equation (equation 7) and differentiating with respect to all joint positions (q_a and q_u), we get

$$\begin{bmatrix} J_\theta & -J_\phi & 0 \\ 0 & -J_\phi & J_\psi \end{bmatrix} \begin{bmatrix} \dot{\theta} \\ \dot{\phi} \\ \dot{\psi} \end{bmatrix} = 0_{6\times 1} \ , \tag{10}$$

where each $J \in \mathbb{R}^{3\times 3}$ is the Jacobian of the corresponding open sub-chain. Expanding this equation is straightforward and will help with the next step. When fully expanded, equation 10 becomes

$$\begin{bmatrix} J_{\theta_{1,1}} & J_{\theta_{1,2}} & J_{\theta_{1,3}} & -J_{\phi_{1,1}} & -J_{\phi_{1,2}} & -J_{\phi_{1,3}} & 0 & 0 & 0 \\ J_{\theta_{2,1}} & J_{\theta_{2,2}} & J_{\theta_{2,3}} & -J_{\phi_{2,1}} & -J_{\phi_{2,2}} & -J_{\phi_{2,3}} & 0 & 0 & 0 \\ J_{\theta_{3,1}} & J_{\theta_{3,2}} & J_{\theta_{3,3}} & -J_{\phi_{3,1}} & -J_{\phi_{3,2}} & -J_{\phi_{3,3}} & 0 & 0 & 0 \\ 0 & 0 & 0 & -J_{\phi_{1,1}} & -J_{\phi_{1,2}} & -J_{\phi_{1,3}} & J_{\psi_{1,1}} & J_{\psi_{1,2}} & J_{\psi_{1,3}} \\ 0 & 0 & 0 & -J_{\phi_{2,1}} & -J_{\phi_{2,2}} & -J_{\phi_{2,3}} & J_{\psi_{2,1}} & J_{\psi_{2,2}} & J_{\psi_{2,3}} \\ 0 & 0 & 0 & -J_{\phi_{3,1}} & -J_{\phi_{3,2}} & -J_{\phi_{3,3}} & J_{\psi_{3,1}} & J_{\psi_{3,2}} & J_{\psi_{3,3}} \end{bmatrix} \begin{bmatrix} \dot{\theta}_1 \\ \dot{\theta}_2 \\ \dot{\theta}_3 \\ \dot{\phi}_1 \\ \dot{\phi}_2 \\ \dot{\phi}_3 \\ \dot{\psi}_1 \\ \dot{\psi}_2 \\ \dot{\psi}_3 \end{bmatrix} = 0_{6\times 1} \ , \tag{11}$$

which can be rearranged into an actuated part, $H_a \in \mathbb{R}^{6\times 3}$, and an unactuated part, $H_u \in \mathbb{R}^{6\times 6}$, such that

$$\begin{bmatrix} H_a(q_a, q_u) & H_u(q_a, q_u) \end{bmatrix} \begin{bmatrix} \dot{q}_a \\ \dot{q}_u \end{bmatrix} = 0_{6\times 1} \ , \tag{12}$$

or equivalently,

$$\dot{q}_u = -H_u^{-1} H_a \dot{q}_a \ . \tag{13}$$

From equation 11, it is apparent that

$$H_a(q_a, q_u) = \begin{bmatrix} J_{\theta_{1,1}} & -J_{\phi_{1,1}} & 0 \\ J_{\theta_{2,1}} & -J_{\phi_{2,1}} & 0 \\ J_{\theta_{3,1}} & -J_{\phi_{3,1}} & 0 \\ 0 & -J_{\phi_{1,1}} & J_{\psi_{1,1}} \\ 0 & -J_{\phi_{2,1}} & J_{\psi_{2,1}} \\ 0 & -J_{\phi_{3,1}} & J_{\psi_{3,1}} \end{bmatrix} \text{, and} \tag{14}$$

$$H_u(q_a, q_u) = \begin{bmatrix} J_{\theta_{1,2}} & -J_{\phi_{1,3}} & -J_{\phi_{1,2}} & -J_{\phi_{1,3}} & 0 & 0 \\ J_{\theta_{2,2}} & -J_{\phi_{2,3}} & -J_{\phi_{2,2}} & -J_{\phi_{2,3}} & 0 & 0 \\ J_{\theta_{3,2}} & -J_{\phi_{3,3}} & -J_{\phi_{3,2}} & -J_{\phi_{3,3}} & 0 & 0 \\ 0 & 0 & -J_{\phi_{1,2}} & -J_{\phi_{1,3}} & J_{\psi_{1,2}} & J_{\psi_{1,3}} \\ 0 & 0 & -J_{\phi_{2,2}} & -J_{\phi_{2,3}} & J_{\psi_{2,2}} & J_{\psi_{2,3}} \\ 0 & 0 & -J_{\phi_{3,2}} & -J_{\phi_{3,3}} & J_{\psi_{3,2}} & J_{\psi_{3,3}} \end{bmatrix} \ , \tag{15}$$

which is, in fact, the constraint Jacobian J_c from the previous section (see equation 9), so the velocities of the unactuated joints are

$$\dot{q}_u = -J_c^{-1} H_a \dot{q}_a \ , \tag{16}$$

assuming J_c is invertible. Observe that $-J_c^{-1} H_a$ is a 6×3 matrix that maps actuated joint velocities to unactuated joint velocities. For example,

$$\dot{\theta}_2 = \begin{bmatrix} 1 & 0 & 0 & 0 & 0 & 0 \end{bmatrix} \left(-J_c^{-1} H_a \right) \dot{q}_a \text{ , and} \tag{17}$$

$$\dot{\theta}_3 = \begin{bmatrix} 0 & 1 & 0 & 0 & 0 & 0 \end{bmatrix} \left(-J_c^{-1} H_a \right) \dot{q}_a \ . \tag{18}$$

We can develop a mapping from the velocities of the actuated joints to the end-effector velocity, using the θ-chain:

$$\begin{bmatrix} \dot{x}_f \\ \dot{y}_f \\ \dot{\measuredangle}_f \end{bmatrix} = J_\theta\left(q_a, q_u\right)\dot{\theta} = J_\theta \begin{bmatrix} & & & \begin{bmatrix}1 & 0 & 0\end{bmatrix} & & \\ \begin{bmatrix}1 & 0 & 0 & 0 & 0 & 0\end{bmatrix} & & & & & \begin{pmatrix}-J_c^{-1}H_a\end{pmatrix} \\ \begin{bmatrix}0 & 1 & 0 & 0 & 0 & 0\end{bmatrix} & & & & & \begin{pmatrix}-J_c^{-1}H_a\end{pmatrix} \end{bmatrix} \dot{q}_a \ , \tag{19}$$

or more simply,

$$\begin{bmatrix} \dot{x}_f \\ \dot{y}_f \\ \dot{\measuredangle}_f \end{bmatrix} = J_{a,\theta}\left(q_a, q_u\right)\dot{q}_a \ , \tag{20}$$

where $J_{a,\theta} \in \mathbb{R}^{3\times 3}$ is the θ-chain *actuator Jacobian*. Similar expressions can be derived for $J_{a,\phi} \in \mathbb{R}^{3\times 3}$ and $J_{a,\psi} \in \mathbb{R}^{3\times 3}$ by returning to equation 16 and deriving expressions for $\dot{\phi}_2$, $\dot{\phi}_3$, $\dot{\psi}_2$, and $\dot{\psi}_3$. Together, the actuator Jacobians are

$$J_{a,\theta} = J_\theta \begin{bmatrix} & & & \begin{bmatrix}1 & 0 & 0\end{bmatrix} & & \\ \begin{bmatrix}1 & 0 & 0 & 0 & 0 & 0\end{bmatrix} & & & & & \begin{pmatrix}-J_c^{-1}H_a\end{pmatrix} \\ \begin{bmatrix}0 & 1 & 0 & 0 & 0 & 0\end{bmatrix} & & & & & \begin{pmatrix}-J_c^{-1}H_a\end{pmatrix} \end{bmatrix} \tag{21}$$

$$J_{a,\phi} = J_\phi \begin{bmatrix} & & & \begin{bmatrix}0 & 1 & 0\end{bmatrix} & & \\ \begin{bmatrix}0 & 0 & 1 & 0 & 0 & 0\end{bmatrix} & & & & & \begin{pmatrix}-J_c^{-1}H_a\end{pmatrix} \\ \begin{bmatrix}0 & 0 & 0 & 1 & 0 & 0\end{bmatrix} & & & & & \begin{pmatrix}-J_c^{-1}H_a\end{pmatrix} \end{bmatrix} \tag{22}$$

$$J_{a,\psi} = J_\psi \begin{bmatrix} & & & \begin{bmatrix}0 & 0 & 1\end{bmatrix} & & \\ \begin{bmatrix}0 & 0 & 0 & 0 & 1 & 0\end{bmatrix} & & & & & \begin{pmatrix}-J_c^{-1}H_a\end{pmatrix} \\ \begin{bmatrix}0 & 0 & 0 & 0 & 0 & 1\end{bmatrix} & & & & & \begin{pmatrix}-J_c^{-1}H_a\end{pmatrix} \end{bmatrix} . \tag{23}$$

2.3.2 Motor sizing

The relationship between joint speeds and end-effector speed is given above in equation 20, but in general, the relationship is

$$V = J_a\dot{\theta} \quad \text{and } \dot{\theta} = J_a^{-1}V \ . \tag{24}$$

Similarly, the relationship between joint torques and end-effector force is

$$\tau = J_a^{\mathrm{T}}F \quad \text{and } F = J_a^{-\mathrm{T}}\tau \tag{25}$$

3 Inverse Kinematics

The inverse kinematics problem is to find joint angles that yield a particular end-effector pose (the foot pose, in the case of this robot). Whereas the forward kinematics for this robot (and closed-chain linkages in general) is difficult to compute, the inverse kinematics can be solved analytically, using basic geometry. In fact, for this particular robot, the foot pose $(x_f, y_f, \measuredangle_f)^{\mathrm{T}}$ itself provides a lot of information: from it, the location of the most distal joint (the "ankle") , with respect to the base frame $\{b\}$, can be calculated as

$$\begin{bmatrix} x_A \\ y_A \end{bmatrix} = \begin{bmatrix} x_f - l_8\cos\measuredangle_f \\ y_f - l_8\sin\measuredangle_f \end{bmatrix} \ , \tag{26}$$

and similarly, the location of the joint above (the "upper ankle") is

$$\begin{bmatrix} x_{uA} \\ y_{uA} \end{bmatrix} = \begin{bmatrix} x_f - (l_7+l_8)\cos\measuredangle_f \\ y_f - (l_7+l_8)\sin\measuredangle_f \end{bmatrix} \ . \tag{27}$$

These two points (the ankle and the upper ankle) are crucial to solving the inverse kinematics because they connect the open subchains, forming closed loops.

3.1 θ-chain inverse kinematics

Knowing the ankle's location, we can analytically solve for θ_1 and θ_2 by applying the same geometric inverse kinematics used with 2R robot arms. Figure 3 below displays most of the geometry relevant for computing θ_1 and θ_2.

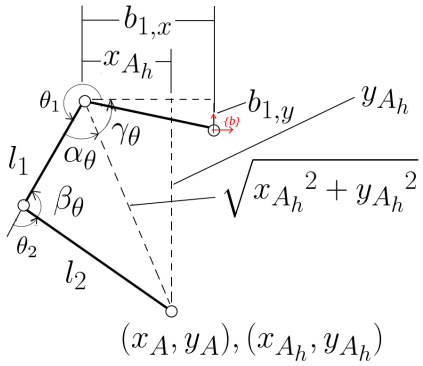

Figure 3: Geometric features relevant for computing inverse kinematics of the θ-chain

First, relative to $\{b\}$, the location of joint θ_1 (the "θ hip") is simply

$$\begin{bmatrix} x_{H,\theta} \\ y_{H,\theta} \end{bmatrix} = \begin{bmatrix} -b_1, x \\ b_1, y \end{bmatrix} .$$

To apply 2R inverse kinematics, we also need the location of the angle with respect to the θ hip:

$$\begin{bmatrix} x_{A_{h,\theta}} \\ y_{A_{h,\theta}} \end{bmatrix} = \begin{bmatrix} -x_{H,\theta} + x_A \\ y_{H,\theta} - y_A \end{bmatrix} .$$

If we draw a line connecting the ankle and the θ hip, the angle between this line and the base frame x-axis is simply

$$\gamma_\theta = \text{atan2}(y_{A_{h,\theta}}, x_{A_{h,\theta}}).$$

Now, the angle between this same line and link l_1 can be found using the Law of Cosines:

$$\alpha_\theta = \arccos\left(\frac{x_{A_{h,\theta}}^2 + y_{A_{h,\theta}}^2 + l_1^2 - l_2^2}{2l_1\sqrt{x_{A_{h,\theta}}^2 + y_{A_{h,\theta}}^2}}\right) ,$$

and the hip angle is

$$\theta_1 = -\gamma_\theta - \alpha_\theta . \tag{28}$$

The (x, y) location of the θ_2 joint (the "knee") can now be computed:

$$\begin{bmatrix} x_{K,\theta} \\ y_{K,\theta} \end{bmatrix} = \begin{bmatrix} x_{H,\theta} + l_1\cos\theta_1 \\ y_{H,\theta} + l_1\sin\theta_1 \end{bmatrix} .$$

We can also find θ_2 by applying the Law of Cosines again:

$$\beta_\theta = \arccos\left(\frac{l_1^2 + l_2^2 - x_{A_{h,\theta}}^2 - y_{A_{h,\theta}}^2}{2l_1 l_2}\right) ,$$

and the knee angle is simply

$$\theta_2 = \pi - \beta_\theta . \tag{29}$$

We can verify the inverse kinematics result by calculating the (x, y) location of the ankle using θ_1 and θ_2:

$$\begin{bmatrix} x_{A,\theta} \\ y_{A,\theta} \end{bmatrix} = \begin{bmatrix} x_{H,\theta} + l_1 \cos\theta_1 + l_2 \cos\theta_1 + \theta_2 \\ y_{H,\theta} + l_1 \sin\theta_1 + l_2 \sin\theta_1 + \theta_2 \end{bmatrix} .$$

Lastly, because we know θ_1, θ_2, and $\measuredangle_f$, we can find θ_3:

$$\theta_3 = \measuredangle_f - \theta_1 - \theta_2 . \tag{30}$$

3.2 ψ-chain inverse kinematics

The inverse kinematics of the ψ-chain mirror those of the θ-chain. Figure 4 below shows the relevant geometric features of the ψ-chain.

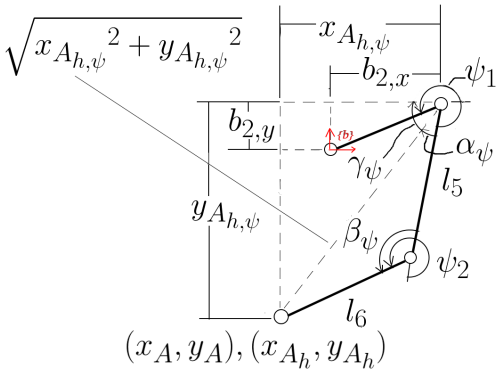

Figure 4: Geometric features relevant for computing inverse kinematics of the ψ-chain

In the $\{b\}$ frame, the origin of the ψ-chain is

$$\begin{bmatrix} x_{H,\psi} \\ y_{H,\psi} \end{bmatrix} = \begin{bmatrix} b_2, x \\ b_2, y \end{bmatrix} ,$$

and with respect to this point, the location of the "ankle" joint is

$$\begin{bmatrix} x_{A_{h,\psi}} \\ y_{A_{h,\psi}} \end{bmatrix} = \begin{bmatrix} x_{H,\psi} - x_A \\ y_{H,\psi} - y_A \end{bmatrix} .$$

The "hip" angle, ψ_1, is given by

$$\gamma_\psi = \text{atan2}(y_{A_{h,\psi}}, x_{A_{h,\psi}}),$$

$$\alpha_\psi = \arccos\left(\frac{x_{A_{h,\psi}}^2 + y_{A_{h,\psi}}^2 + l_5^2 - l_6^2}{2 l_5 \sqrt{x_{A_{h,\psi}}^2 + y_{A_{h,\psi}}^2}} \right) ,$$

$$\psi_1 = \pi + \gamma_\psi + \alpha_\psi . \tag{31}$$

The "knee" angle, ψ_2, is given by

$$\beta_\psi = \arccos\left(\frac{l_5^2 + l_6^2 - x_{A_{h,\psi}}^2 - y_{A_{h,\psi}}^2}{2 l_5 l_6} \right) ,$$

$$\psi_2 = \pi + \beta_\psi . \tag{32}$$

The "ankle" angle, ψ_3, is simply

$$\psi_3 = \measuredangle_f - \psi_1 - \psi_2 . \tag{33}$$

3.3 ϕ-chain inverse kinematics

Just as a 2R arm has "elbow-up" and "elbow-down" configurations, this planar robot has a number of possible configurations for the same end-effector pose. One such example is the "elbow-left" or "elbow-right" configuration of the ϕ chain. The derivations below assume the "elbow-left" configuration, so the equations resemble those of the θ chain (the "elbow-right" configuration equations resemble those of the ψ-chain).

This model defines the origin of the $\{b\}$ frame at joint ϕ_1, so

$$\begin{bmatrix} x_{H,\phi} \\ y_{H,\phi} \end{bmatrix} = \begin{bmatrix} 0 \\ 0 \end{bmatrix} \ .$$

The "ankle" of the ϕ chain is different from that of the θ and ψ chains and is consequently referred to as the "upper ankle". Repeating the same geometric procedure as done above for the other two chains, we first calculate the "hip" angle, ϕ_1:

$$\gamma_\phi = \text{atan2}(y_{uA}, x_{uA}),$$

$$\alpha_\phi = \arccos\left(\frac{x_{uA}^2 + y_{uA}^2 + l_3^2 - l_4^2}{2l_3\sqrt{x_{uA}^2 + y_{uA}^2}}\right) ,$$

$$\phi_1 = -\gamma_\phi - \alpha_\phi \ . \tag{34}$$

The "knee" angle, ϕ_2, is given by

$$\beta_\phi = \arccos\left(\frac{l_3^2 + l_4^2 - x_{uA}^2 - y_{uA}^2}{2l_3 l_4}\right) \ ,$$

$$\phi_2 = \pi - \beta_\phi \ . \tag{35}$$

The "ankle" angle, ϕ_3, is simply

$$\phi_3 = \measuredangle_f - \phi_1 - \phi_2 \ . \tag{36}$$

References

[1] K. M. Lynch and F. C. Park. *Modern Robotics.* Cambridge University Press.